Chain Flexibility Effect on the Refractive Index Grating of Fully Functionalized Carbazole/DO3/Epoxy Polymer

CHI JUNG CHANG,[1] WHA TZONG WHANG,[1] KEN YUH HSU[2]

[1] Department of Materials Science and Engineering, National Chiao-Tung University, 1001 Ta Hsueh Road, Hsinchu 300, Taiwan, Republic of China

[2] Institute of Electro-Optical Engineering, National Chiao-Tung University, 1001 Ta Hsueh Road, Hsinchu 300, Taiwan, Republic of China

Received 8 June 1998; accepted 15 December 1998

ABSTRACT: The photorefractive (PR), photoconductive, and holographic characteristics of 3-amino-9-ethyl carbazole (AEC)/dispersed orange 3 (DO3)/diepoxy main chain copolymers are investigated to study the relationship between the structure and properties. The recorded pattern exhibits good fringe contrast with the resolution 20 μm in the recorded hologram. The formation rate of refractive index grating (PR grating) can be speeded up by applying an electric field or changing comonomer structure or monomer composition. Faster PR response can be achieved by incorporating aliphatic diepoxy with longer chain length or increasing the concentration of the charge transport moieties, while more nonlinear optical (NLO) segment (DO3) in the copolymer results in higher diffraction efficiency. The dark decay rate of the PR film at room temperature depends on the dark conductivity and steric interaction between the NLO chromophores and the polymer matrix. However, the latter shows greater influence on the dark decay at elevated temperature. More charge transport segment increases the dark conductivity and it leads to higher dark decay rate. The diffracted signals of polymers synthesized from the diepoxy comonomers containing longer soft chain exhibit slower dark decay at room temperature, but drop sharply as the temperature get higher. In comparison with experimentally measured dark decay at elevated temperature, thermal stimulated current spectroscopy is a more sensitive tool than differential scanning calorimetry diagrams to evaluate what temperature a sharp dark decay of the PR signal will occur. © 1999 John Wiley & Sons, Inc. J Appl Polym Sci 74: 1321–1333, 1999

Key words: holographic recording; photorefractive; polymer; 3-amino-9-ethyl carbazole; dispersed orange 3

INTRODUCTION

Organic photorefractive (PR) materials have held public attention since they were discovered[1] in 1991. PR polymers have been developed for applications to optical computing[2], optical correlation[3], data storage,[4,5] or image storage[6]. A large portion of the reported PR polymers were made of a photoconducting polymer matrix [usually the photoconductor poly-(N-vinylcarbazole)(PVK)] doped with nonlinear optical (NLO) molecules[7–16]. Since the glass transition temperature (T_g) of PVK is as high as 200°C, Bolink and coworkers[17] incorporated an additional plasticizer into the PVK-based PR polymer to enhance the PR performance by increasing the chain mobility of the doped

Correspondence to: W. Whang.

Contract grant sponsor: National Science Council, Republic of China; contract grant number: NSC 87–2216-E009–002.

Journal of Applied Polymer Science, Vol. 74, 1321–1333 (1999)

 CCC 0021-8995/99/061321-13

NLO molecules. Volodin and coworkers[6] studied a new doped polymer composite having unique performances in the dynamic holography and image storage. The composite was made of the PVK doped with a charge transfer molecule, an NLO azo dye, and a plasticizer. It showed a high PR efficiency, good sensitivity, and reasonably fast response time. However, two problems were encountered when the plasticizer was added the crystallization tendency of the NLO molecules increased and the dielectric breakdown voltage of the PR film decreased. These problems limit the concentration of the plasticizer. To increase the segment mobility and to prevent the film from crystallization at the same time, fully functionalizing all components onto a polymer is a better way to solve these two problems. The hologram images were written and read without the external electric field to prevent the film from the dielectric breakdown.

In this study, we try to solve these two problems by synthesizing a fully functionalized PR polymer. Both the charge transporting (CT) moieties and NLO moieties are copolymerized with the diepoxy comonomers. The orientational mobility of the NLO moieties can be adjusted by changing the chemical structure of the diepoxy comonomers. The relative concentrations of the NLO and the CT moieties are also adjusted to study the dependence of the composition on the photoconductive and the PR characteristics. After a hologram image is recorded, the PR medium is kept in the dark and the diffraction signal may decay gradually. For long-term data storage in a PR medium, in addition to promoting the quality of the recorded hologram, such as resolution and contrast properties, the dark decay should be as low as possible to extend the storage life. Therefore, the relationships among the dark current, the chemical structure, the composition, and the dark decay behaviors at the room temperature are investigated. We want to find a way to prepare a PR polymer that can fit the requirement of certain applications. Dark decay behaviors at elevated temperatures are studied by both the experimentally measured diffracted signals and the thermal stimulated current (TSC) measurement.

EXPERIMENTAL

The charge generation moiety 3-amino-9-ethyl carbazole (AEC), the NLO azo dye dispersed orange 3 (DO3), and diepoxy comonomers were added to cyclohexanone in a three-necked round-bottomed flask under nitrogen atmosphere. After these solids dissolved completely, a diepoxy comonomer was added to the solution. Three different aliphatic diepoxy comonomers including diepoxy butane (DEB); 1,2,7,8-diepoxyoctane (DEO); and 1,4-butanediol diglycidyl ether (BDE) were used in the preparation of the copolymers with a solid content of 30 wt. The reaction mixture is refluxed at 105°C for 12 h and then vacuum dried. The chemical structures of the polymers are illustrated in Figure 1. The dried polymers were ground to powder and then dissolved in cyclohexanone. The polymer films were prepared by spin coating the polymer solution onto the indium-tin oxide (ITO) side of an ITO glass. After the films were vacuum dried, two resulting films were hot pressed in the vacuum oven and the polymer was sandwiched between two ITO layers.

Degenerate four-wave mixing (FWM) as shown in Figure 2 was used to measure the PR properties. A green beam laser (λ = 514 nm) and a red beam laser (λ = 632.8 nm) were applied as the writing and reading beams, respectively. The writing beam is expanded by a beam expander and then split into two writing beams that are mutually coherent and are s-polarized. They are spatially overlapped in the polymer film with an angle of 20°to form a diffraction grating. The reading beam is p-polarized and is counterpropagating to one of the writing beams at the Bragg matching condition. The diffracted signal is detected by a photodetector.

Figure 3 illustrates the experimental set-up used for the holographic recording and readout. A green light laser (λ = 514 nm) is used as the light source. During holographic recording, the beam is expanded by a beam expander and then split into two writing beams, beam 1 and beam 2, by a polarization beam splitter. A half-wave plate is used to rotate the polarization state of beam1 so that the two beams are s-polarized. Beam 1 illuminates the center part of a test chart, and then the pattern is imaged onto the PR polymer film. Beam 2 is incident on the polymer film at an angle of 30°. The average power density measured at the polymer plane is about 14 mW/cm^2. After the hologram is recorded, beam 1 is cut and the hologram image is read out by beam 2. The restored image is imaged onto a charge-couple device (CCD) camera. The hologram images are recorded without applying electric fields on the polymer film.

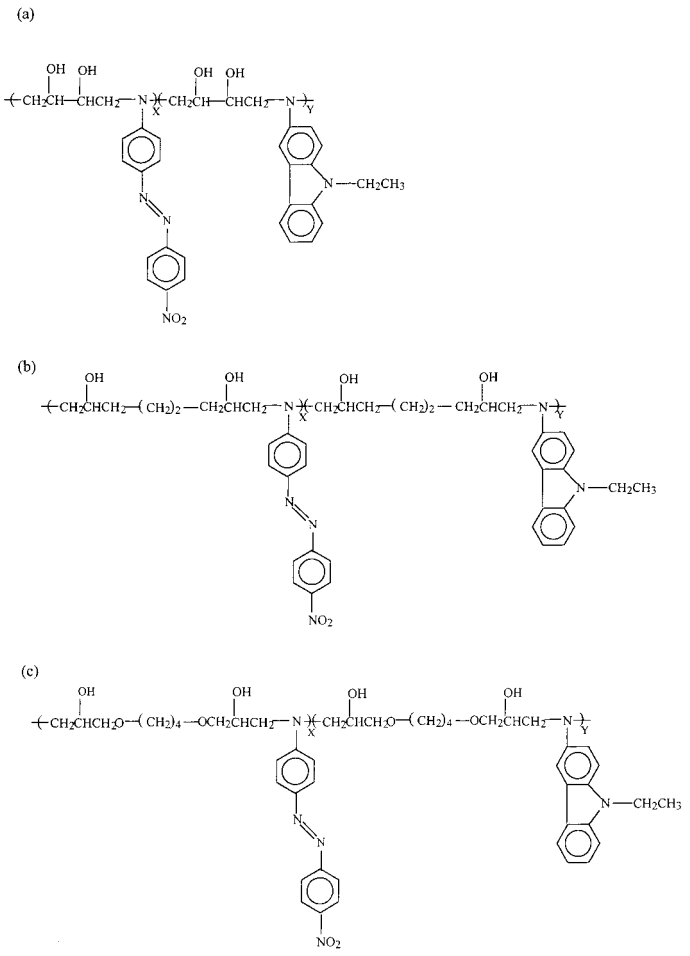

Figure 1 The chemical structure of (a) DEB/AEC/DO3, (b) DEO/AEC/DO3, and (c) BDE/AEC/DO3.

All TSC measurements are obtained with a Solomat TSC/RMA 9100 spectrometer. To obtain the TSC spectra, all films are poled by a constant static electric field (E = 100 V/mm) at T_p for 5 min. T_p is set at a temperature 5 to 10° higher than the T_g. The films are then quenched down to

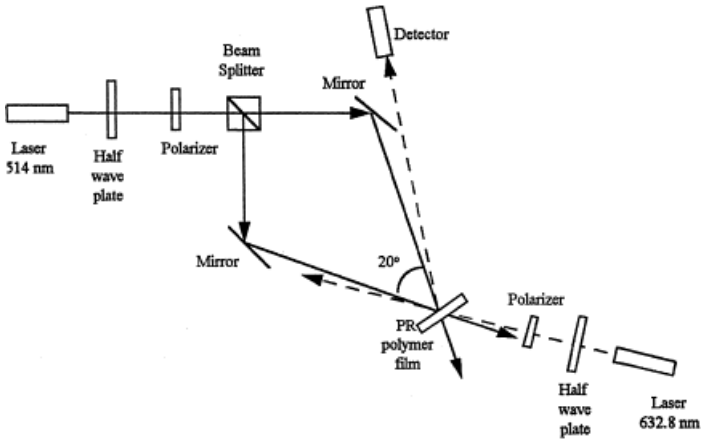

Figure 2 Experimental setup of the degenerate FWM measurement.

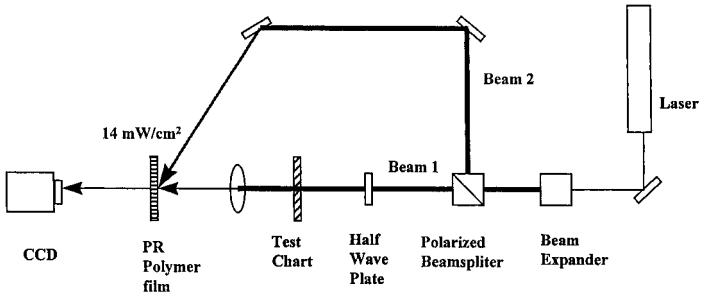

Figure 3 The experimental setup used for the holographic recording and readout.

a freezing temperature T_f (−100°C) to freeze the dipole orientation under the electric field for 5 min. After the field is removed, the depolarization current of the sample is measured by heating it at 7°C/min from T_f to final temperature T_e ($T_e \geqq T_p$). The differential scanning calorimetry (DSC) measurements are achieved with a DuPont 2910 thermal analysis system and are performed from room temperature to the final temperature at a heating rate of 10°C/min.The UV/vis spectra are obtained with a Hitachi U2000 spectrometer. The Fourier transform infrared (FTIR) spectra are measured by a Nicolet Protege 460 spectrometer.

For the photoconductivity measurement, the surface of the PR polymer film spin coated onto the ITO glasses is vapor-deposited with gold. A green beam laser (λ = 514 nm) is chosen as the light source to measure the photoconductivity of the polymer under the fixed applied field (300V) except the 1,4-butanediol diglycidyl ether (BDE)/AEC/DO3 (2 : 1.50 : 0.5) film (120V). The thickness of the films is 15μm.

RESULTS AND DISCUSSION

UV/vis and FTIR spectra can provide the structural information of these PR polymers. The UV/vis absorption spectra are shown in Figure 4. It is seen that the absorption peaks of AEC and DO3 monomers are at 350 and 435 nm, respectively. All the PR polymer films prepared with different diepoxy comonomers show an absorption peak at about 495 nm, which is due to the absorption of the azo chromophore DO3, and another peak at 320 nm, which is resulted from the carbazole unit of AEC. A distinct red shift on the absorption peak of the azo moiety DO3 and a blue shift peak on the absorption peak of AEC moiety are observed in the polymer.

The FTIR spectra of the PR polymers are shown in Figure 5; there is no C—O—C absorption of the epoxy ring in the 1198–1176 cm^{-1} region . The broad absorption of the hydroxyl group between 3200 and 3650 cm^{-1} and the C—N absorption of tertiary amine at 1334 cm^{-1} implies that AEC and DO3 are chemically bonded onto the polymer chain by the reaction between the amine and epoxy groups. In addition, there are the N—N stretching vibration at 1429 cm^{-1} and the NO_2 vibration absorption at 1500 cm^{-1} due to the DO3 moiety.

DSC diagrams of different PR polymers are illustrated in Figure 6. The T_g of the BDE/AEC/DO3 polymer films are 44°C and 48°C for the composition 2 : 0.5 : 1.5 and 2 : 1 : 1, respectively. Note that the copolymer of BDE/AEC/DO3 (2 : 1.5 : 0.5) has a T_g at 68°C, which is the highest of

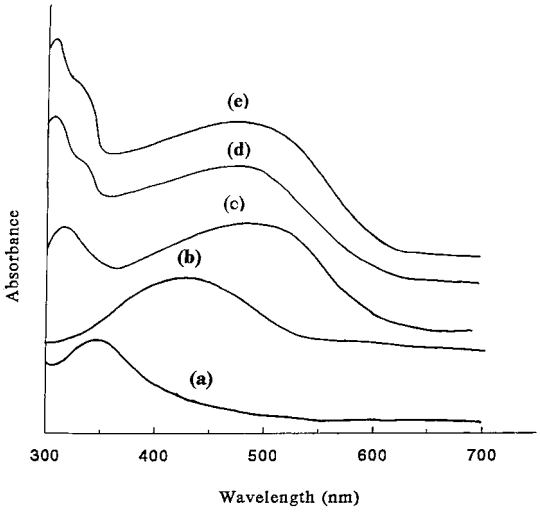

Figure 4 The UV/vis absorption spectra of (a) AEC in cyclohexanone, (b) DO3 in cyclohexanone, (c) BDE/AEC/DO3 film, (d) DEO/AEC/DO3 film, and (e) DEB/AEC/DO3 film.

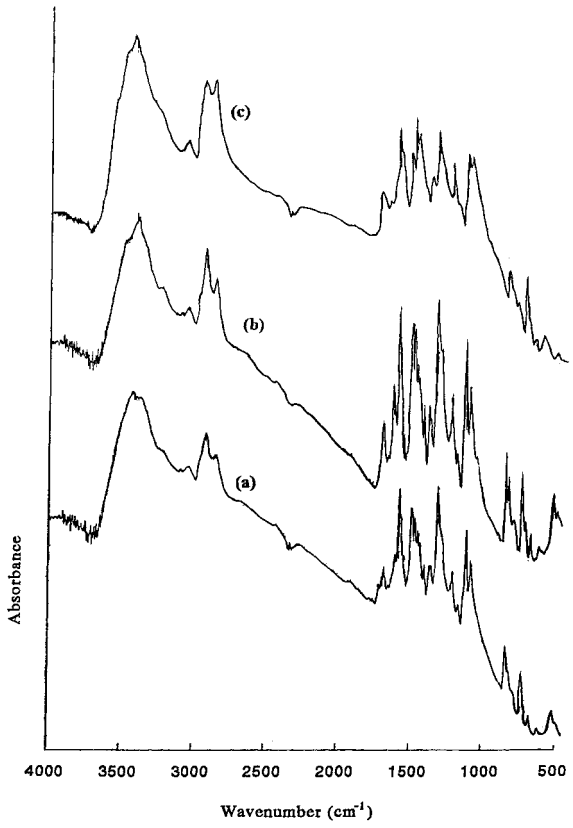

Figure 5 The FTIR spectra of (a) DEB/AEC/DO3, (b) DEO/AEC/DO3, and (c) BDE/AEC/DO3.

these copolymers. DEO/AEC/DO3 (2 : 1 : 1) and DEB/AEC/DO3 (2 : 1 : 1) have T_g at 52°C and 58°C, respectively, which is higher than that of the corresponding BDE/AEC/DO3 film. The data show that the shorter the chain length of the comonomer, the higher the transition temperatures are measured for the greater steric hindrance between the pendent side moieties.

Figure 7 shows the time dependence of the diffracted signal in FWM experiments under different external electric fields. The rise time (T_r) is defined as the time needed for the diffracted signal to rise from 10 to 90% of the saturation value during writing; the decay time (T_d) is defined as the time required for the diffracted signal to drop from 90 to 10% of the saturation value during erasure. The electric field dependence of T_r, T_d, and the diffraction efficiency of the BDE/AEC/DO3 film is illustrated in Table I. When no electric field is applied, the photogenerated charge could be separated and transported only by the diffusion process due to the gradient of carrier density. Not only the grating growth rate is slow but also the diffraction efficiency is low. After an external electric field is applied, the photogenerated charges can be separated and transported by both the diffusion and the drift processes. There-

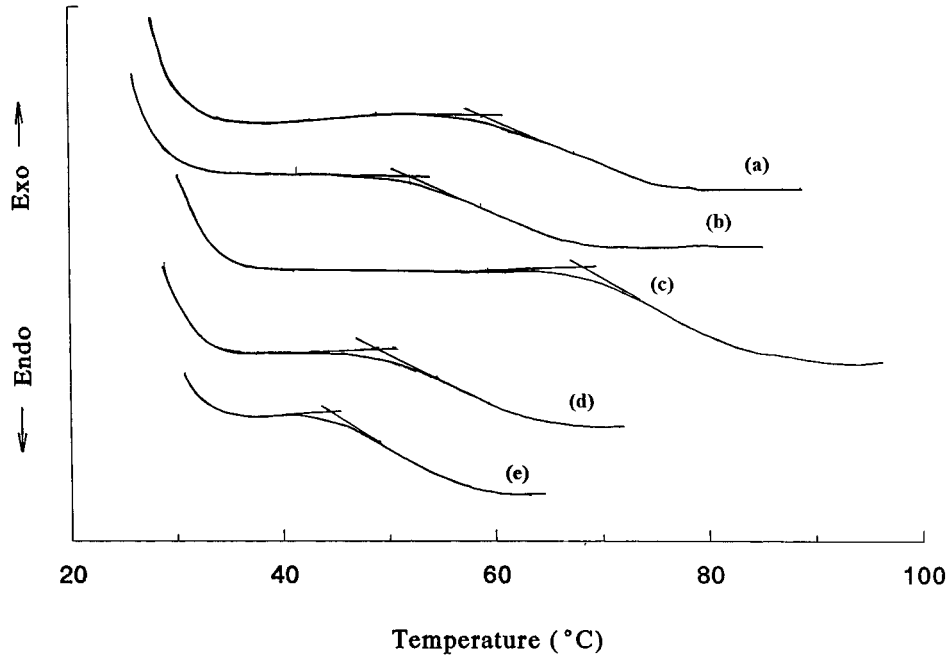

Figure 6 DSC of (a) DEB/AEC/DO3 (2 : 1 : 1), (b) DEO/AEC/DO3 (2 : 1 : 1), (c) BDE/AEC/DO3 (2 : 1.5 : 0.5), (d) BDE/AEC/DO3 (2 : 1 : 1), and (e) BDE/AEC/DO3 (2 : 0.5 : 1.5).

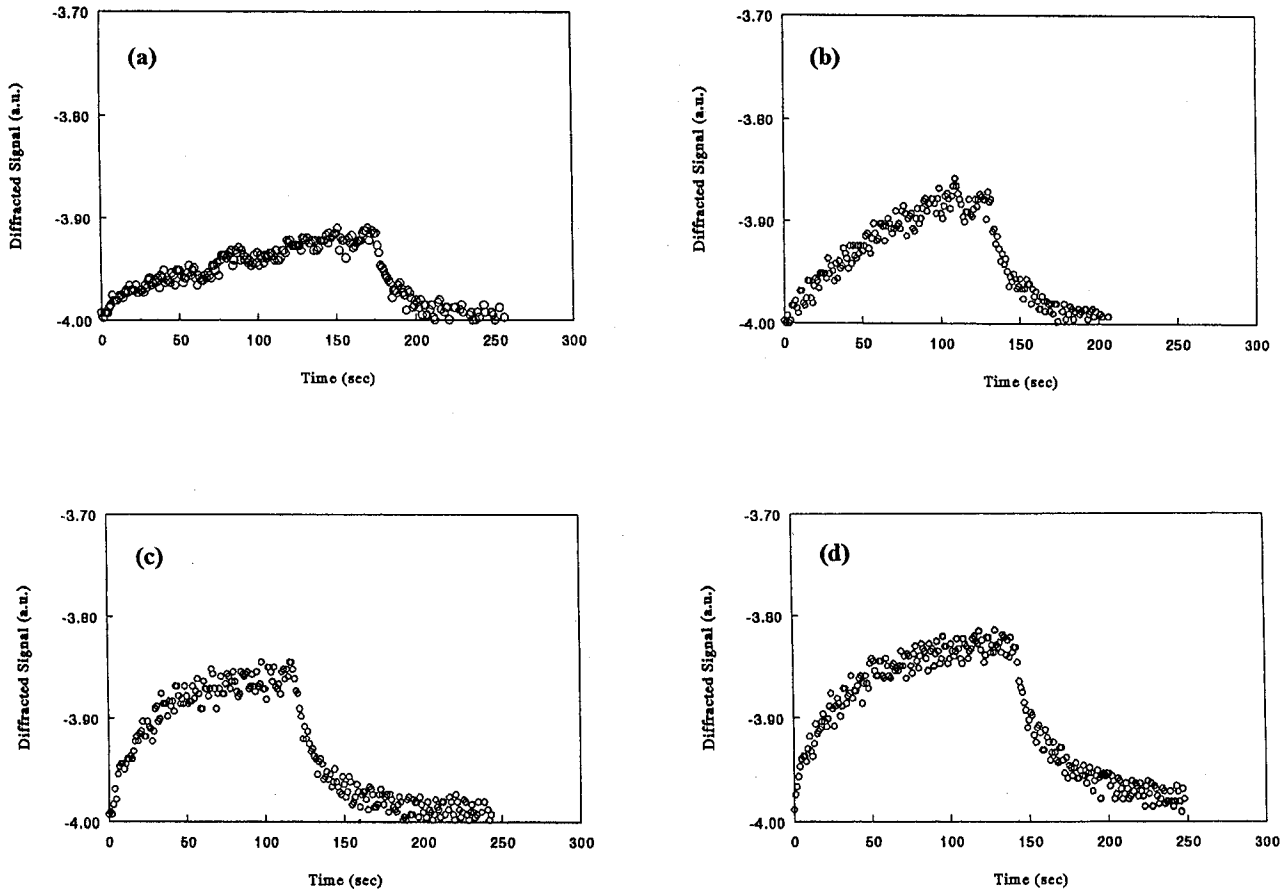

Figure 7 The time dependence of the FWM diffracted signal of the BDE/AEC/DO3 (2 : 1 : 1) film measured under different external electric field: (a) no electric field, (b) 4 V/μm, (c) 10 V/μm, and (d) 20 V/μm.

fore, the grating growth rate becomes faster, and the diffraction efficiency is a little bit higher.

To evaluate the resolution of the reconstructed hologram images recorded in the PR film, a resolution test chart is utilized. Except for the group number, the chart is correspondent to the United States Air Force's (USAF) 1951 resolution target standard. For example, the fifth group in this test chart is equal to the third group of the USAF resolution target standard, and the forth group in this test chart is equal to the s group of the USAF resolution target standard, and so on. Figure 8(a) shows the image of the original resolution chart. Figure 8(b and c) illustrate the reconstructed images of the resolution chart, which are written in the DEO/AEC/DO3 film with an exposure time of 60 and 150 s, respectively. Figure 8(d and e) show a reconstructed image that is written in the BDE/

Table I The Electric Field (E) Dependence of the Rise Time (T_r), the Decay Time (T_d), and the Diffraction Efficiency (η) of the BDE/AEC/DO3 (2 : 1 : 1) Film

E (V/μm)	0	4	10	20
T_r (sec)	175	81	56	54
T_d (sec)	130	45	42	41
η	1.4×10^{-3}	1.6×10^{-3}	1.7×10^{-3}	2.0×10^{-3}

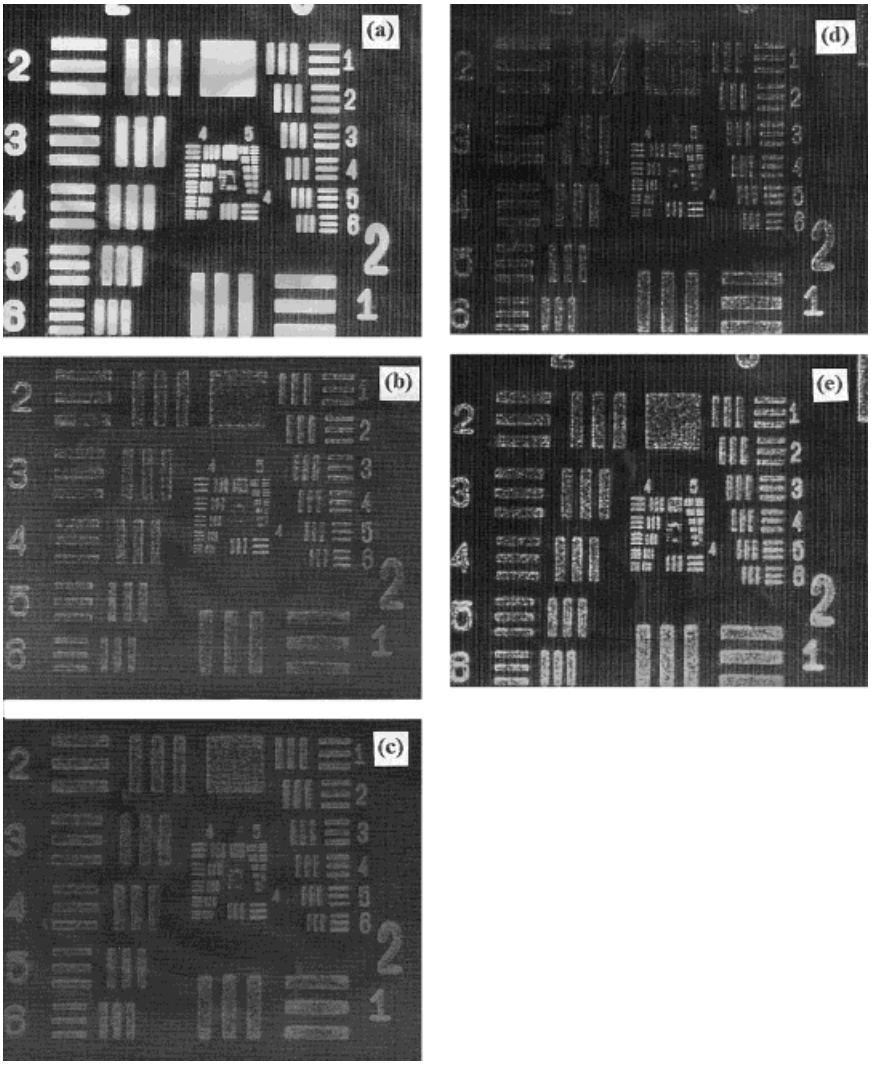

Figure 8 The image of (a) the original resolution chart transmitting through a filter, a reconstructed image of (b) the resolution chart written in the DEO/AEC/DO3 film for 60 and (c) 150 s, and a reconstructed image (d) written in the BDE/AEC/DO3 film for 60 and (e) 150 s.

AEC/DO3 film with an exposure time of 60 and 150 s, respectively. In Figure 8(a), the fourth element of the fifth group is resolvable. The corresponding element is perceptible in the restored image, as shown in Figure 8(b). The recorded image was more clear when the recording time reached 150 s. The hologram growth rate is slower than that of the doped polymeric system.

Table II Photorefractive Properties of the BDE/AEC/DO3 Film with Different Molar Ratio

	BDE/AEC/DO3 2 : 1.5 : 0.5	BDE/AEC/DO3 2 : 1 : 1	BDE/AEC/DO3 2 : 0.5 : 1.5
T_r (sec)	5	175	300
T_d (sec)	4	130	360
η	5.3×10^{-5}	1.4×10^{-3}	3.2×10^{-3}

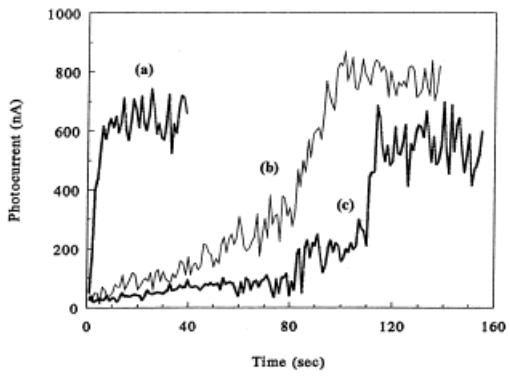

Figure 9 Photocurrents of BDE/AEC/DO3 films with the BDE : AEC : DO3 ratio (a) 2 : 1.5 : 0.5, (b) 2 : 1 : 1, and (c) 2 : 0.5 : 1.5 as a function of exposure time.

Since the image demagnification is two in our optical system, the resolution of the recorded hologram is about 20 μm.

The response time and the diffraction efficiency of BDE/AEC/DO3 films with different monomer ratio are shown in Table II. It is found that more CT segments lead to faster PR response, while more NLO segments lead to higher diffraction efficiency. Both the NLO segments and the CT segments are chemically bonded by the comonomers; they compete with each other for the volume fraction. Increasing the concentration of NLO segments will not only dilute the CT segments, but also make them farther apart from each other. Farther distance may halt the conduction of the carriers. And the PR response becomes slower when the AEC concentration gets lower.

Photocurrents of BDE/AEC/DO3 polymer films with different BDE : AEC : DO3 ratios as a function of exposure time is illustrated in Figure 9. The BDE/AEC/DO3 film with the component ratio 2 : 1.5 : 0.5 exhibits the fastest photoconductive response among these three PR polymers. It takes 5 s for the diffraction signal to reach its saturation value under an external electric field of 8 V/μm. It is seen that as the AEC content decreases, the photoconductive response gets slower. As the concentration of the NLO segments gets higher, the diffraction signal of the film with the component ratio 2 : 1 : 1 saturates after exposure for 100 s under a higher external electric field of 20 V/μm. When the component ratio becomes 2 : 0.5 : 1.5, it is found that not only the time needed for saturation gets longer (120 s) but also the current turns lower. However, the diffraction efficiency of the BDE/AEC/DO3 (2 : 0.5 : 1.5) film is about one hundred times larger than that of the BDE/AEC/DO3 (2 : 1.5 : 0.5) film because more NLO chromophores are available.

Table III shows the response time and the diffraction efficiency of the PR films synthesized from comonomers with different chain lengths at the same molar ratio 2 : 1 : 1 (comonomer: AEC : DO3) under zero electric field. DEB comonomer possesses the shortest chain length. BDE owns the longest chain among the three, and its C–O–C segments inside the molecule make it more flexible. The DEO/AEC/DO3 polymer synthesized from a longer diepoxy chain exhibits a faster PR response in comparison with the DEB/AEC/DO3 polymer. Since AEC and DO3 are transversely bonded onto the polymer backbone through a diepoxy comonomer, a longer chain diepoxy comonomer makes AEC and DO3 further apart from each other. It also provides the pendent NLO chromophore larger flexibility and at the same time decreases the steric hindrance for orientation and thus promotes the response speed. Comparing BDE/AEC/DO3 and DEO/AEC/DO3 films, it is shown that further increasing the chain length of the diepoxy comonomer decreases the PR response speed. In addition to the orientational feasibility of NLO chromophores, the chain length also affects the charge transport phenomena. Figure 10 shows the time dependence of photocurrents of the three films. There is a tendency that the photoconductive response speed gets slightly slower as the chain length of the diepoxy comonomer increases. As the chain length becomes longer, the charge transport segments are further apart from each other and the

Table III Photorefractive Properties of the BDE/AEC/DO3, DEO/AEC/DO3, and DEB/AEC/DO3 Films with the Molar Ratio Diepoxy AEC : DO3 = 2 : 1 : 1

	BDE/AEC/DO3	DEO/AEC/DO3	DEB/AEC/DO3
Tr (sec)	175	105	>600
T_d (sec)	130	90	>275
η	1.4×10^{-3}	1.3×10^{-3}	$>1.7 \times 10^{-3}$

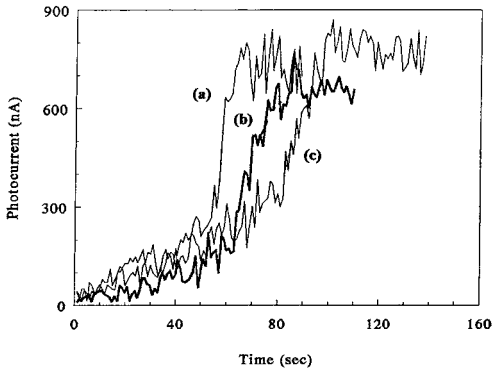

Figure 10 The time dependence of photocurrents of the (a) DEB/AEC/DO3, (b) DEO/AEC/DO3, and (c) BDE/AEC/DO3 film with the same molar ratio 2 : 1 : 1 after exposure.

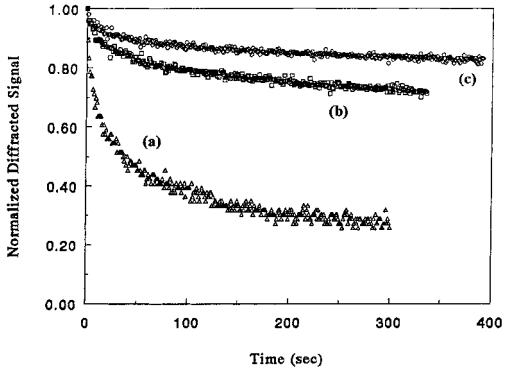

Figure 12 The dark decay of PR gratings in BDE/AEC/DO3 films with the BDE : AEC : DO3 ratio (a) 2 : 1.5 : 0.5, (b) 2 : 1 : 1, and (c) 2 : 0.5 : 1.5.

transport of photogenerated charges becomes harder. This causes a decrease in the photoconductivity and thus offsets the chain flexibility that is favorable to the PR response.

The asymmetric two-beam coupling is shown in Figure 11. Samples were previously irradiated to produce deep trap sites in the polymer, which can enhance the modulated space charge field. It is a process referred to as the optical trap activation[18]. An increase in the intensity of beam 1 is observed after beam 2 is blocked. It is complemented with an approximately equal decrease in the intensity of beam 2 when beam 1 is blocked. The coupling gain is small because of the strong absorption at the wavelength 514 nm.

The dark decays of PR gratings in BDE/AEC/DO3 polymers with different molar ratios are demonstrated in Figure 12. The diffracted signal of BDE/AEC/DO3 (2 : 1.5 : 0.5) drops to 30% of the original value during the dark decay process in 5 min. The final diffracted signals of BDE/AEC/DO3 (2 : 1 : 1) and BDE/AEC/DO3 (2 : 0.5 : 1.5) films drop to 72 and 82% of the original value in the dark decay. The final normalized signal of BDE/AEC/DO3 is much lower than that of the other two films. That is, higher AEC content leads to faster dark decay. The dark conductivities of these three films are shown in Figure 13, which shows that the dark conductivity increases as the content of charge transport segment AEC increases. This means that increasing the content of the charge transport segment favors the formation of charge transport pathways in the polymer films. The dark decay of PR gratings in BDE/AEC/DO3, DEO/AEC/DO3, and DEB/AEC/DO3 polymers with the same component molar ratio (2 : 1 : 1) are depicted in Figure 14. The normalized final diffracted signal of BDE/AEC/DO3 is the highest of all, and that of DEB/AEC/DO3 is the lowest. Figure 15 indicates that there is no sig-

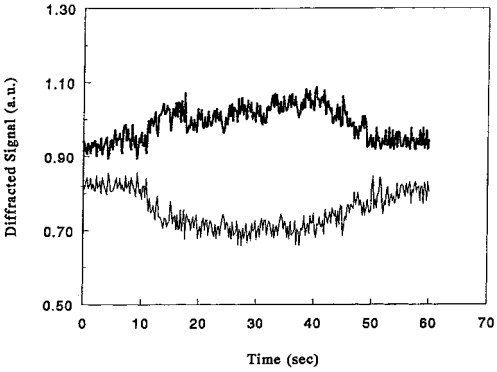

Figure 11 Asymmetric two-beam coupling of the BDE/AEC/DO3 (2 : 1 : 1) film.

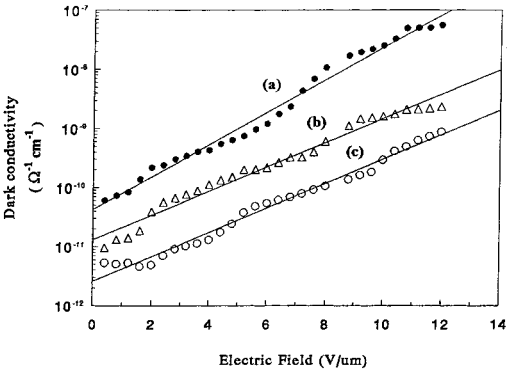

Figure 13 The dark conductivity of BDE/AEC/DO3 films with the BDE : AEC : DO3 ratio (a) 2 : 1.5 : 0.5, (b) 2 : 1 : 1, and (c) 2 : 0.5 : 1.5.

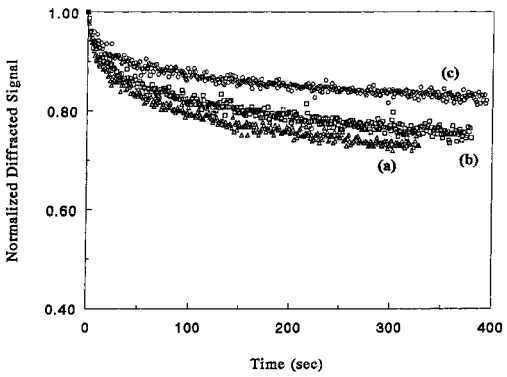

Figure 14 The dark decay of PR gratings in (a) DEB/AEC/DO3, (b) DEO/AEC/DO3, and (c) BDE/AEC/DO3 films with the same component molar ratio 2 : 1 : 1.

nificant difference in the dark conductivity of these three films. We attribute the difference in the dark decay behavior to the relaxation of NLO segments. A confined elastic model[19] used in clarifying the interaction between NLO chromophores and the polymer matrix can be chosen to explain this phenomena. In this model, NLO chromophores are considered to be embedded in polymer cavities. At low temperatures, the embedded NLO chromophores cannot freely rotate in a polymer matrix. In the fully functionlized PR polymer system, the NLO chromophores are elastically tied to the local polymer matrix at the temperature below T_g. The local relaxation motion of the NLO chromophore may be impeded by steric interaction with the polymer matrix. Since DEB has the shortest chain length among these PR polymers, those pendent AEC and DO3 segments of the DEB/AEC/DO3 polymer lie much closer than those of DEO/AEC/DO3 and BDE/AEC/DO3, and the cavity in DEB/AEC/DO3 may be the smallest. The NLO segments are aligned by the induced space charge field after writing. Since the NLO chromophores encounter larger steric hindrance during the orientation on writing, it generates a greater elastic recovery force between the NLO chromophores and the matrix after writing. When both writing beams are cut, there are greater recovery forces for the NLO chromophores to return to their original status, and the final diffracted signal of the DEB/AEC/DO3 film drops faster than the other two films in darkness. As the chain length of the diepoxy comonomer increases, the PR copolymer chain becomes softer and the distance between NLO chromophores and adjacent pendent moieties increases. Thus, the cavity becomes larger, and the steric interaction between the NLO chromophores decreases. The elastic recovery force decreases as the chain length of the diepoxy increases. Therefore the dark decay becomes slower, and the final normalized diffraction signals become higher when the diepoxy comonomer with longer chain length is used.

Tsutsumi and colleagues[20] used the TSC measurement to study the orientational relaxation of transversely aligned nonlinear optical dipole moments to the main backbone at elevated temperatures. Since NLO segments are bonded to the fully functionalized PR polymer and the orientational relaxation of the NLO chromophores leads to the decay of PR diffraction signal, the TSC technique can also be used to evaluate the decay of the PR signal at elevated temperatures. In the writing period of FWM measurement, the NLO chromophores are poled by the space charge field. The disorientation of the chromophores results in the decay of the grating. A similar process occurred in the TSC measurement. The dipoles of the film are poled in a constant applied electric field at the poling temperature and then quenched to the freezing temperature. As the temperature increases, the current can be detected once certain aligned dipoles are disoriented. Figure 16 shows the TSC curves of PR films. Figure 16(a and b) show a transition peak at 65°C for the PR copolymer DEB/AEC/DO3 (2 : 1 : 1) and a peak at 61°C for the polymer DEO/AEC/DO3 (2 : 1 : 1), respectively. However, Figure 16(c) shows two peaks at 50 and 56°C for the BDE/AEC/DO3 (2 : 1 : 1) PR polymer. Because of larger chain length and flexible C–O–C segments in the BDE diepoxy comonomer, the NLO moiety in the PR polymer can be disoriented at a temper-

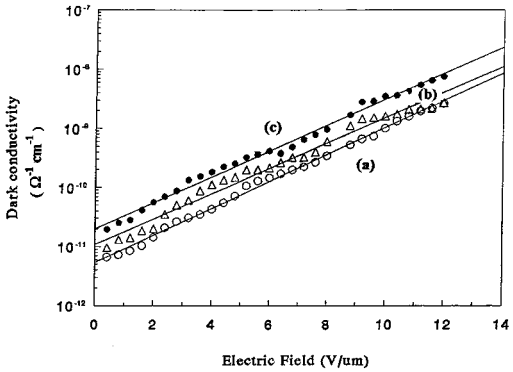

Figure 15 The dark conductivity of (a) DEB/AEC/DO3, (b) DEO/AEC/DO3, and (c) BDE/AEC/DO3 films with the same component molar ratio 2 : 1 : 1.

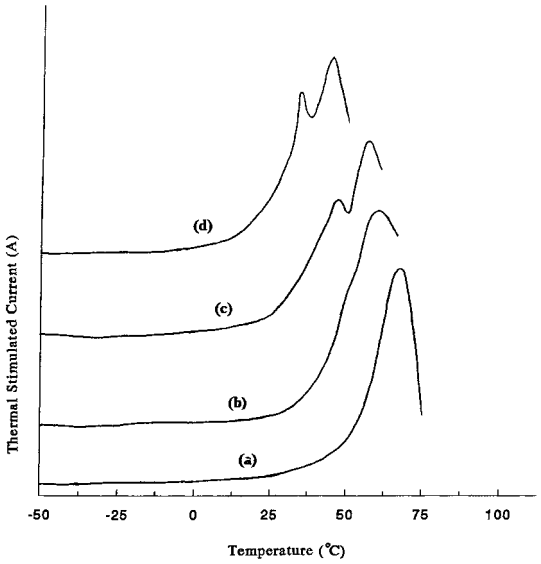

Figure 16 TSC curves of (a) DEB/AEC/DO3(2 : 1 : 1), (b) DEO/AEC/DO3(2 : 1 : 1), (c) BDE/AEC/DO3 (2 : 1 : 1), and (d) BDE/AEC/DO3 (2 : 0.5 : 1.5) films.

ature 50°C below the T_g at 56°C in this polymer. The low temperature peak relates to the randomization of the oriented NLO chromophores, and the high temperature peak corresponds to the segmental motion of the polymer at T_g. The TSC curve of BDE/AEC/DO3 (2 : 0.5 : 1.5) film in Figure 16(d) shows two peaks at 38°C and at 47°C, respectively. The transition peaks shift to lower temperatures as the concentration of DO3 increases due to increasing the intermolecular spacing by incorporating more NLO long segments.

As shown in Figure 6, the T_g can be obtained from the DSC spectra. However, Figure 16 reveals that, in addition to T_g, β transition peak can be observed in the TSC spectra of some films (BDE/AEC/DO3 copolymer). To investigate the dark decay behavior near the β transition temperature and the T_g, the decay of the diffracted signal is measured in the dark by heating the films stepwise. Two kinds of films are chosen. One is the BDE/AEC/DO3 (2 : 0.5 : 1.5) film with both the β transition and the glass transition. The other type includes the DEB/AEC/DO3 (2 : 1 : 1) film and the DEO/AEC/DO3 (2 : 1 : 1) film exhibiting only the glass transition. The dark decay signals of the three films at elevated temperatures are illustrated in Figure 17. In Figure 17(c), the temperature of the BDE/AEC/DO3 (2 : 0.5 : 1.5) film is raised by 7°C per step. The diffracted signal gets lower when the temperature is raised from 25 to 32°C. When the temperature reaches 39°C, a temperature near the β transition temperature (38°C), a sharp drop of the signal is observed. This may result from the disorientation of the NLO side chain moiety. As the temperature is heated to 46°C, a temperature near the T_g

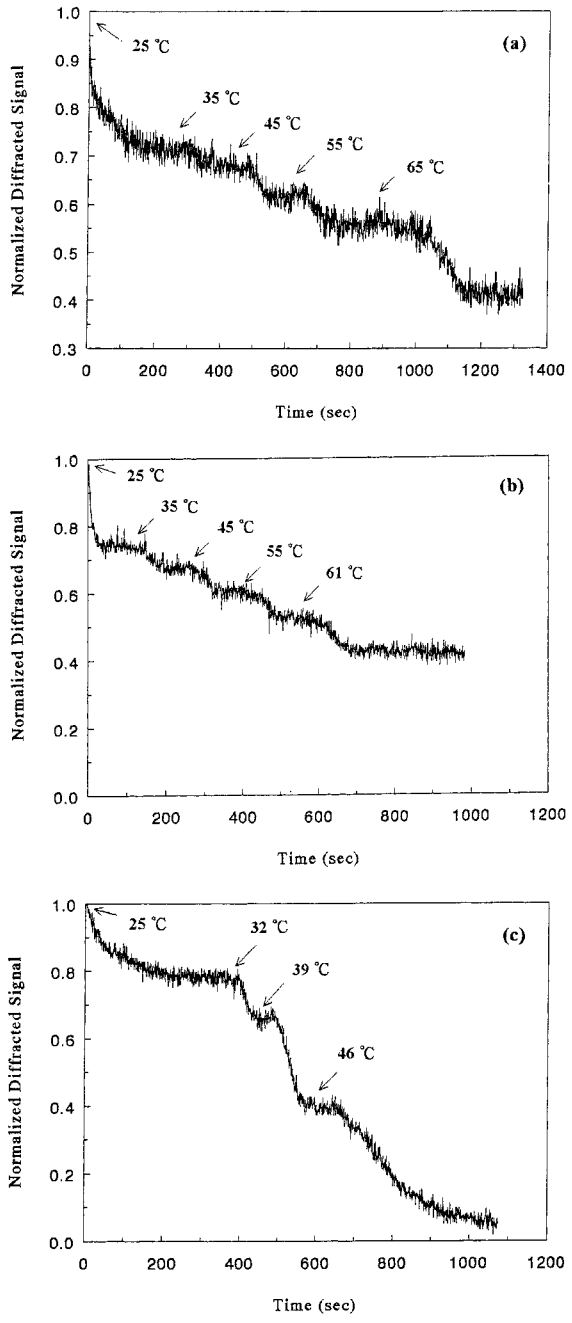

Figure 17 Dark decay of normalized diffracted signal of (a) DEB/AEC/DO3 (2 : 1 : 1), (b) DEO/AEC/DO3 (2 : 1 : 1), and (c) BDE/AEC/DO3 (2 : 0.5 : 1.5) films during the heating process.

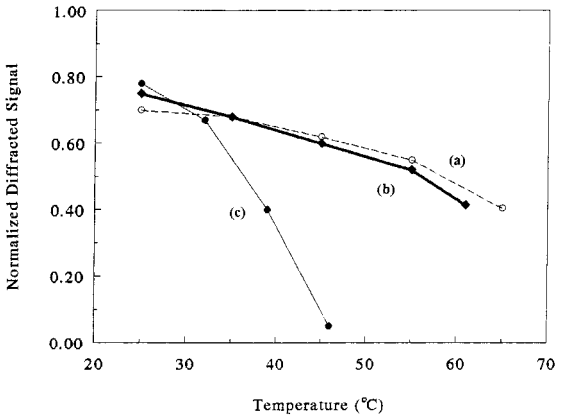

Figure 18 Dark decay of normalized diffracted signal of (a) DEB/AEC/DO3 (2 : 1 : 1), (b) DEO/AEC/DO3 (2 : 1 : 1), and (c) BDE/AEC/DO3 (2 : 0.5 : 1.5) films at different temperatures.

(47°C), the signal drops to only 5% of the original value. Because the BDE/AEC/DO3 film consists of a relatively flexible mainchain segment, the temperature shows a relatively significant influence on the dark decay behavior. For the DEO/AEC/DO3 (2 : 1 : 1) film [Fig. 17(b)], the dark decay rate of diffraction signal is relatively slow when the film is heated stepwise. The extent of decrease in the latter film is much less than that observed in the former. No sharp drop is observed in the DEO/AEC/DO3 film until the temperature is elevated near T_g. Similar results are observed in the DEB/AEC/DO3 (2 : 1 : 1) film. The temperature-dependent dark decay properties are clearer when the normalized steady dark decay signal of the PR films versus the temperature is plotted in Figure 18. All films show a large decrease of the diffraction signal near T_g. For films with the β transition, such a sharp decrease will occur at even lower temperature near the β transition temperature. Since TSC is more sensitive than DSC to the β transition, TSC is a better technique to use in studying the thermal stability of the PR signal of the polymeric PR material.

CONCLUSIONS

This study has provided a new type of PR copolymer with the azo dye and carbazole moieties. Both are transversely attached onto the polymer backbone. The PR properties can be measured under zero electric field. The response speed is adjustable. Three methods are feasible to speed up the response, including applying an electric field, incorporating diepoxy comonomers with longer chain length, and changing the relative component concentrations. With the same relative component concentration, polymers synthesized from comonomers with longer chain length exhibit faster PR response than that from shorter depoxy comonomers. This is due to the enhanced orientational mobility of NLO chromophores. Changing the relative component compositions shows that more charge transport segments lead to faster PR response, while more NLO segments lead to higher diffraction efficiency. When an electric field is applied, the grating growth rate becomes faster and the diffraction efficiency gets higher. Potential application in the holographic information storage has been demonstrated. Hologram images can be written and read out from the copolymer by a low-power laser under a zero external electric field. The resolution of the recorded hologram is about 20 μm with good fringe contrast. The dark decay rate of the PR film at room temperature depends on the dark conductivity and the steric interaction between the pendent NLO chromophores and the polymer matrix. However, the steric interaction shows greater influence on the dark decay behavior at elevated temperatures. More charge transport segments increase the dark conductivity and lead to higher dark decay rate. The diffracted signals of polymers synthesized from the longer soft diepoxy comonomers exhibit slow dark decay at room temperature. However, the diffraction signal of the long PR polymer drops more significantly than that of the short PR polymer as the temperature increases. At the temperature near T_g, all films show a sharp decrease in the diffraction signal. For films with a β transition, such a sharp decrease in the diffracted signal will occur at an even lower temperature near the β transition temperature. Since TSC is more sensitive than DSC to the β transition, TSC spectroscopy is used to evaluate at what temperature a sharp dark decay of the PR signal will occur.

The authors would like to acknowledge the financial support from the National Science Council of the Republic of China. The authors thank M. Hsieh for her kind help in the hologram recording experiment.

REFERENCES

1. Ducharme, S.; Scott, J. C.; Twieg, R. J.; Moerner, W. E. Phys Rev Lett 1991, 66, 1846.

2. Halvorson, C.; Kraabel, B.; Heeger, A. J.; Volodin, B. L.; Meerholz, K.; Sandalphon, N.; Peyghambarian, N. Opt Lett 1995, 20, 76.
3. Vacar, D.; Heeger, A. J.; Volodin, B.; Kippelen, B.; Peyghambarian, N. Rev Sci Instrum 1997, 68, 1119.
4. Heanue, J. F.; Bashaw, M. C.; Hesselink, L. Science 1994, 265,749.
5. Lundquist, P. M.; Poga, C.; DeVoe, R. G.; Jia, Y.; Moerner, W. E.; Bernal, M. P.; Coufal, H.; Grygier, R. K.; Hoffnagle, J. A.; Jefferson, C. M.; Macfarlane, R. M.; Shelby, R. M.; Sinserbox, G. T. Opt Lett 1996, 21, 890.
6. Volodin, B. L.; Sandalphon, N.; Meerholz, K.; Kippelen, B.; Kukhtarev, N. V.; Peyghambarian, N. Opt Eng 1995, 34, 2213.
7. Zhang, Y.; Cui, Y.; Prasad, P. N. Phys Rev B 1992, 46, 9900.
8. Donckers, M. C. J. M.; Silence, S. M.; Walsh, C. A.; Hache, F.; Burland, D. M.; Moerner, W. E.; Twieg, R. J. J Opt Lett 1993, 18, 1044.
9. Silence, S. M.; Hache, F.; Donckers, M.; Walsh, C. A.; Burland, D. M.; Bjorklund, G. C.; Twieg, R. J.; Moerner, W. E. Proc Soc Photo Opt Instrum Eng 1993, 1852, 253.
10. Silence, S. M.; Donckers, M. C. J. M.; Walsh, C. A.; Burland,D. M.; Twieg, R. J.; Moerner, W. E. Appl Opt 1994, 33, 2218.
11. Zhang, Y.; Spencer, C. A.; Ghosal, S.; Casstevens, M. K.; Burzynski, R. Appl Phys Lett 1994, 64, 1908.
12. Zhang, Y.; Spencer, C. A.; Ghosal, S.; Casstevens, M. K.; Burzynski, R. J Appl Phys 1994, 76, 671.
13. Malliaras, G. G.; Krasnikov, V. V.; Bolink, H. J.; Hadziioannou, G. Appl Phys Lett 1994, 66, 262.
14. Meerholz, K; Volodin, B. L.; Sandalphon, N.; Kippelen, B.; Peyghambarian, N. Nature, 1994, 371, 497.
15. Kippelen, B.; Sandalphon, N.; Meerholz, K.; Volodin, B. L.; Lyon, S. R.; Padias, A. B.; Hall, Jr., H. K.; Peyghambarian, N. Mater Res Soc Proc 1994, 328, 577.
16. Moerner, W. E.; Silence, S. M. Chem Rev 1994, 94, 127.
17. Bolink, H. J.; Krasnikov, V. V.; Malliaras, G. G.; Hadziioannou, G. J Phys Chem 1996, 100, 16356.
18. Silence, S. M.; Bjorklund, G. C.; Moermer, W. E. Opt Lett 1994, 19, 1822.
19. Liao, C. L.; Huang, J. Y.; Chang, C. J.; Whang, W. T. Nonlinear Optics 1995, 12, 309.
20. Tsutsumi, N.; Matsumoto, O.; Sakai, W. Macromolecules 1997, 30, 4584.